JOURNAL OF MATERIALS SCIENCE 24 (1989) 14–22

Review

High temperature oxidation of low alloy steels

YAO-NAN CHANG, FENG-I WEI
Research and Development Department, China Steel Corporation, Hsiao Kang, Kaohsiung, Taiwan

This is a review paper of high temperature (greater than 200° C) oxidation of steels with total alloying elements less than 3 wt%. Topics include the iron–oxygen phase diagram, the oxidation mechanism and kinetics as well as the effects of alloying elements, environmental atmospheres, and cold work.

1. Introduction

Low alloy steels play an important role in structural applications as they cost much less than high alloy steels and non-ferrous alloys. However, oxidation often causes serious problems in high temperature environments. Furthermore, in manufacturing processes, scaling always occurs on steels after forging, hot rolling, heat treatment, and subsequent cooling. In addition to the deterioration of the base metals, the properties of the scale on the surface also affect the descaling problem for cold rolling or other further applications. Therefore, it is necessary to understand such behaviours. This paper discusses the high temperature oxidation properties of low alloy steels from the iron–oxygen phase diagram, the oxidation mechanism and kinetics. Thereafter, the effects of alloying elements, environmental atmospheres, and cold work are summarized. High temperature here is taken to mean in excess of 200° C below which the oxidation rates are usually not appreciable [1, 2]. Low alloy steels are steels with total alloying elements less than 3 wt %. Carbon steels and such dilute iron–base alloys are also included for reference.

2. Iron–oxygen phase diagram

Fig. 1 is the Fe–O phase diagram at 1 atm [3]. It is evident that three kinds of oxides wüstite (FeO), magnetite (Fe_3O_4), and haematite (Fe_2O_3) might exist at temperatures greater than 570° C. Below this temperature, only Fe_3O_4 and Fe_2O_3 exist, while FeO is unstable. However, this diagram only represents equilibrium conditions which in practice may not always occur. With the addition of alloying elements, the simple diffusion pattern (see Fig. 2 below) may be modified and the full range of oxides that might be possible at a particular temperature will not be observed even though they would be thermodynamically stable, i.e. kinetics usually affects their formation.

The wüstite formed at high temperature is actually expressed as $Fe_{1-x}O$ which implies an iron-deficient crystal structure. The value of x increases with the distance from the scale-base metal interface. Normally wüstite possesses 5–16% of such defects. Below 570° C, it will decompose via the following steps

$$(1-4y)Fe_{1-x}O \rightarrow (1-4x)Fe_{1-y}O + (x-y)Fe_3O_4$$

$$x > y$$

$$4Fe_{1-y}O \rightarrow Fe_3O_4 + (1-4y)\alpha\text{-Fe}$$

Thus the total reaction is

$$4Fe_{1-x}O \rightarrow Fe_3O_4 + (1-4x)\alpha\text{-Fe}$$

The optimum temperature to attain the maximum reaction rate reported by Chaudron and Forestier [4] is 470° C, while that reported by Fisher *et al.* [5, 6] is 400° C. This difference, of course, comes from different oxidation and decomposition atmospheres.

Over the range 200–570° C, iron forms a two-layer oxide scale consisting of an inner layer of Fe_3O_4 and an outer slightly thinner layer of Fe_2O_3. The oxidation rate of iron, of course, increases with temperature.

Above 570° C, the oxidation of iron shows a marked increase. The three oxides exist simultaneously on the iron substrate: an adherent layer of FeO overlaid with an Fe_3O_4 layer and an outer Fe_2O_3 layer. Whilst the growth rate of FeO is high due to its large defect concentration and this oxide is sufficiently plastic at high temperature to maintain contact with the receding metal surface, the ratio of thickness of the three layers claimed to be independent of time and temperature has been reported in references [7] and [8] as $FeO:Fe_3O_4:Fe_2O_3 = 100:10:1$ and $100:5:1$ respectively.

When the temperature is raised still further, scale might soften or melt, and combustion occurs. FeO does not melt until 1369° C, while the melting point of Fe_3O_4 is 1594° C [9]. Above 1380° C, Fe_2O_3 will dissociate in air because its dissociation pressure is greater than 0.21 atm [10]. Of course, dissociation occurs at a lower temperature provided Fe_2O_3 is heated in lower oxygen partial pressure.

3. Oxidation mechanism and kinetics

The mechanism of iron oxidation given by Hauffe [11] is commonly accepted as shown in Fig. 2, although the temperature is just above 600° C. In Fig. 2,

$$\text{(I)}\quad Fe \rightarrow Fe^{2+}(FeO) + 2e^-(FeO)$$

0022-2461/89 $03.00 + .12

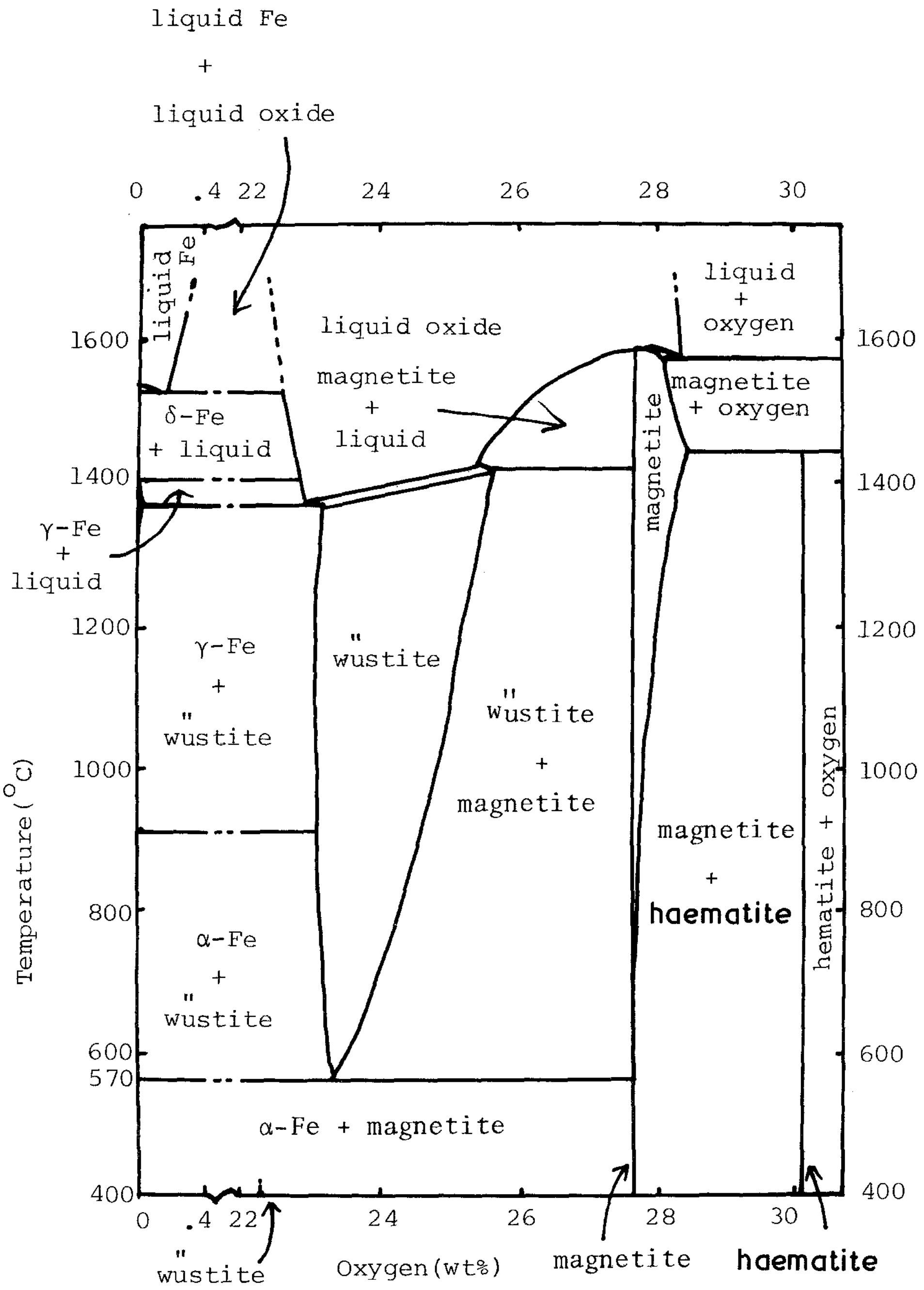

Figure 1 Fe–O phase diagram at 1 atm [3].

$$\text{(II)}\ Fe^{2+}(FeO) + 2e^-(FeO) \rightarrow Fe^{2+}(Fe_3O_4) + 2e^-(Fe_3O_4)$$

$$Fe^{2+}(FeO) + 2e^-(FeO) + Fe_3O_4 \rightarrow 4FeO$$

$$Fe^{2+}(FeO) + 2e^-(FeO) + O^{2-}(Fe_3O_4) + 2\oplus(Fe_3O_4) \rightarrow FeO$$

$$\text{(III)}\ Fe^{2+}(Fe_3O_4) + 2e^-(Fe_3O_4) + 2Fe^{3+}(Fe_2O_3) + 6e^-(Fe_2O_3) + 4O^{2-}(Fe_2O_3) + 8\oplus(Fe_2O_3) \rightarrow Fe_3O_4$$

$$2Fe_3O_4 + O^{2-}(Fe_2O_3) + 2\oplus(Fe_2O_3) \rightarrow 3Fe_2O_3$$

$$O^{2-}(Fe_2O_3) + 2\oplus(Fe_2O_3) \rightarrow O^{2-}(Fe_3O_4) + 2\oplus(Fe_3O_4)$$

$$\text{(IV)}\ 1/2O_2 \rightarrow O^{2-}(Fe_2O_3) + 2\oplus(Fe_2O_3)$$

where e^- is an electron and $\oplus$ is an electron hole. The above reactions indicate that iron oxidation consists mainly of the outward diffusion of iron ions and the inward diffusion of oxygen ions. Gesmundo and Viani [12] proposed that the formation of FeO and Fe_3O_4 is mainly controlled by the outward diffusion of iron ions, while that of Fe_2O_3 is by the inward diffusion of oxygen ions. However, if there are dislocation pipes, grain boundaries, or microcracks, Hauffe's model should be modified by Rahmel's model [13] which suggests that the inward diffusing species are oxygen molecules rather than oxygen ions.

As of other metals or alloys, high temperature oxidation of low alloy steels can be thought of as a series of four stepwise processes [14], and the slowest step is the rate-controlling step. Therefore, one can understand the principal mechanism from the measurement of the kinetic process. Experience has shown that essentially three types of rate laws are observed in high temperature oxidation: parabolic, linear, and intermediate. If diffusion process in the oxide is the rate-controlling step, then oxidation rate obeys a parabolic

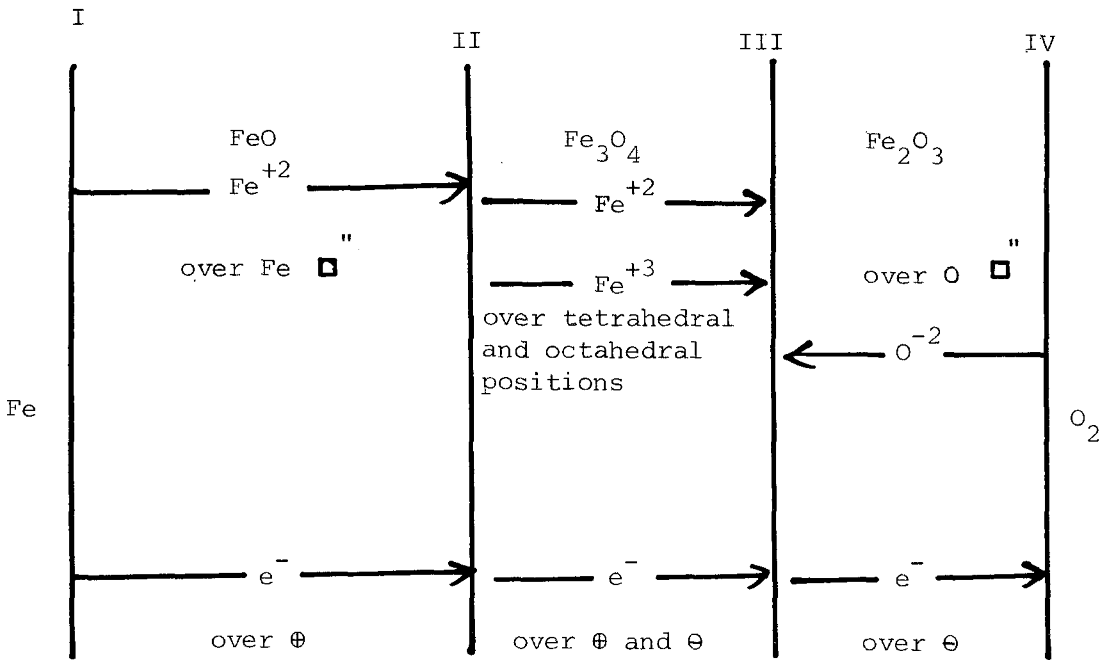

Figure 2 The oxidation mechanism of iron above 600° C after Hauffe [11]. □ vacancy in lattice, ⊕ electron hole, ⊖ over charged electron, □″ vacancy either excess negative charge.

rate law. If the metal surface or the phase boundary interface reaction is the rate-controlling step, then oxidation obeys a linear rate law. In addition, the logarithmic or exponential rate laws usually represent the initial stages of oxidation or low temperature ($<200°$ C) rates only [14, 15].

4. Effect of alloying elements on the oxidation

4.1. Carbon

The main effect of carbon on the oxidation rates is to make them more erratic. Carbon diffuses to the scale–base metal interface and reacts with iron oxide to evolve CO gas and develop a gap. In high carbon steel at high temperature, the gas pressure in the gaps may cause gross cracking so that the atmosphere gains access to the core and the oxidation rate is increased. However, if the scale does not crack, the stabilization of the gaps may hinder the outward diffusion of iron ions and result in a slower oxidation rate. However, if the gaps contain sufficient amount of CO gas, they will facilitate oxygen transport and result in a higher oxidation rate.

For example, Boggs and Kachik [16] found that the oxidation rate of Fe–C alloy in 10 torr O_2 at 500° C increased when its carbon content increased from zero to 0.99 wt %. Caplan *et al.* [17] also found that Fe–0.5 wt % C and Fe–1.0 wt % C alloys oxidized faster than Fe–0.1 wt % C alloy in 1 atm O_2 at 500° C. They explained that this phenomenon is largely due to gap formation between oxide and metal. That is, if carbon is present in sufficient concentration to precipitate as cementite, then the cementite–ferrite interphase boundaries of pearlite will provide sinks for the cation vacancies from decarburization, whereas over the ferrite the vacancies will condense to form a gap and hinder the transfer of iron ions into the scale. On the other hand, the oxidation rates of Fe–0.5 wt % C alloy and Fe–1.0 wt % C alloy in 1 atm oxygen at 700° C were slower than that of pure iron [18]. Malik and Whittle [19] also found that Fe–C alloys with 0.1 to 1.2 wt % C oxidized slower than pure iron in 1 atm oxygen at 600 to 850° C. It was proposed [18] that a residue of graphite from the oxidation of Fe_3C is left at the scale–base metal interface causing poor contact between the scale and the base metal, while at 500° C, the system is Fe–Fe_3O_4–Fe_2O_3 rather than Fe–FeO–Fe_3O_4–Fe_2O_3. Grain boundary diffusion of carbon in Fe_3O_4 and Fe_2O_3 may be adequate to remove graphite from the interface.

However, above 570° C, the oxidation rate does not always decrease monotonically with increasing carbon content. One should consider what kind of phase exists at the oxidation temperature from the Fe–C phase diagram and the solubility of carbon in that phase. For example [19], at 850° C the oxidation rate is 0 wt % C > 0.4 wt % C > 1.2 wt % C > 0.8 wt % C > 0.1 wt % C, because the 0.1 wt % C alloy consists of the $\alpha + \gamma$ phases, the 0.4 wt % C and 0.8 wt % C alloys of the γ phase, and the 1.2 wt % C alloy, γ + Fe_3C. It is presumably easier for rejected carbon to be incorporated into the 0.4 wt % C alloy since the γ phase is considerably undersaturated with respect to carbon. There is thus less separation of the scale from the alloy, less magnetite in the scale and consequently a higher overall oxidation rate. Although the 0.8 wt % C alloy also consists of γ, it is relatively close to the saturation limit. The 0.1 wt % C and 1.2 wt % C alloys already contain, at least, one phase which is saturated with carbon and thus can only accommodate excess carbon by changing the relative proportions of the two phases. However, Wei *et al.* [20] found that carbon steel with 0.82 wt % C oxidized slower than that with 0.06 wt % C in air at 700 to 900° C. The investigation of Korochkin *et al.* [21] indicated that the effect of carbon content (0.07

to 0.84 wt %) on the oxidation of steel in air at 800 to 1200° C passed through a minimum loss at 0.3 to 0.5 wt % C. Both of these phenomena were not explained.

In general, if carbon hinders the transport of iron ions or oxygen ions, its effect is to reduce the oxidation rate. On the other hand, if it facilitates the transport, it will increase the oxidation.

4.2. Aluminium

Addition of aluminium to iron reduces the oxidation rate through the formation of an aluminium-rich layer at the scale–base metal interface and the retardation of iron ion diffusion. The exact nature of such aluminium-rich layer appears to vary with the aluminium content of the steel, the temperature, and the oxidizing atmosphere. For example [22], the aluminium-rich layer was probably Al_2O_3 after the oxidation of Fe–1 wt % Al alloy in 1 atm O_2 at 500 to 700° C, and such layer was $FeAl_2O_4$ spinel after the oxidation in the same atmosphere at 700–900° C. In general, the scales formed on aluminium-containing low alloy steels consist of outer iron-rich layers and inner aluminium-rich layers. However, at low temperature up to 500° C, very dilute Fe–Al alloys (< 0.5 wt % Al) [23] showed slightly higher oxidation rate than iron by doping the p-type semiconducting iron oxide (Fe^{2+} deficit) with Al^{3+} causing an increase in the cation vacancy concentration and thereby the diffusion rate, while in concentrated alloys the amount of Al^{3+} was in excess of doping the cation vacancies and the aluminium-rich layer could be formed. At higher temperatures the oxidation rate of such dilute alloys was considerably reduced presumably due to the enhanced diffusion rate of aluminium and the more rapid formation of the aluminium-rich layer. With steels which form protective layers, the oxidation kinetics was initially parabolic but the oxidation rate ultimately decreased and deviated from the parabolic law as the aluminium-rich layer became established [22, 24].

Another oxidation resistant mechanism is to increase the temperature of wüstite formation. For example [25], the temperature of wüstite formation in the steel containing 1.8 wt % Al was found to be 798° C rather than 570° C from the Fe–O phase diagram, and the diffusion of iron in magnetite is slower than that in wüstite, although the enrichment of alloying element on the surface of the steel also contributed to the oxidation resistance.

4.3. Silicon

Similar to Fe–Al alloys, protection of Fe–Si alloys arises from preferential formation of silicon-rich layer at the scale–base metal interface due to its less noble behaviour than iron. Dilute Fe–Si alloys were subject to internal oxidation [24] and complex scales were found. An SiO_2-rich inner scale layer apparently formed with alloys containing 2 to 3 wt % Si or more [26] and this transition from internal to external SiO_2 formation might result in a markedly reduced oxidation rate. The slower oxidation rate was probably due to the lower diffusion rate of silicon through the oxide layers and the hindered iron ion diffusion through the SiO_2 layer. However, in air at 500 and 700° C, the maximum oxidation resistance of silicon steel with 0 to 3 wt % Si was achieved at 2 wt % Si [24]; the reason is not yet clear.

The minimum bulk concentration of silicon to form a continuous SiO_2 film can be predicted from the atmosphere theoretically. For example [27], in CO_2 + 1 vol % CO at 500° C, such minimum silicon content is 2.6 wt %. In low alloys, the SiO_2 formed at the scale–base metal interface (or internal SiO_2) may ultimately react with FeO to form the spinel fayalite (Fe_2SiO_4) as found by Tuck [28]. Smeltzer *et al.* [29] oxidized an Fe–1.52 wt % Si alloy in CO/CO_2 atmosphere at 890 to 1000° C. Under these conditions the only iron oxide formed was FeO. The scale consisted of an external compact layer of FeO and an inner Fe_2SiO_4–FeO conglomerate. The spinel is less protective than SiO_2 and has a lower melting point which limits the upper temperature stability limit of dilute Fe–Si alloys to 1150° C [23].

In comparison with aluminium and chromium (see below). Addition of silicon has the greatest effect on the oxidation resistance at 500 and 700° C [24] due to its more protective property than aluminium and its rather higher diffusion rate than chromium in iron (causing earlier formation of protective layer). The effect of silicon in Fe–Al–Si alloys is to establish a silicon-rich oxide layer outside or in the outer region of the aluminium-rich oxide layer. The scale formed is inherently more protective than the purely aluminium-containing scale. However, aluminium is still helpful in retarding the advance of the oxidation front into the metal and permitting silicon to be oxidized to reinforce protection. von Fraunhofer and Pickup [24] also found that in air at 500 and 700° C Fe–1 wt % Al–1 wt % Si alloy oxidized much slower than Fe–2 wt % Al–2 wt % Si alloy and Fe–2 wt % Si alloy. The former phenomenon is because the high aluminium content interferred with or even prevented the oxidation of silicon. Therefore, the scale on the Fe–2 wt % Al–2 wt % Si alloy was less protective due to the absence of silicon. The latter phenomenon was explained by the inversion effect, i.e. the corrosion resistance in air falls off rapidly if the aluminium : silicon ratio deviates from 1 : 1.

Furthermore, the oxidation of mild steel in high pressure CO_2 at high temperature is characterized by three distinct regimes [30]: an initial protective period during which the kinetics is approximately parabolic; a transitional stage and a non-protective oxidation during which the kinetics is linear. Jepson *et al.* [31] found that additions of 0.41 to 0.43 wt % Si were extremely effective in prolonging the time for the onset of non-protective behaviour at 520° C. Their explanation attributes to the oxidation of silicon to silicate which is stable within the oxide for longer time (at least up to 10 000 in their study).

4.4. Chromium

The major protection action of chromium is also due to the formation of chromium-containing layer at the scale–base metal interface. Wood *et al.* [32]

reported that additions of 0.16 to 0.2 wt % Cr to iron increased the initial oxidation rate in oxygen at 1000° C, probably because Cr^{3+} ions increased the number of cation vacancies in the major phase FeO similar to the doping mechanism of p-type semiconducting iron oxide with Al^{3+} described above. However, the rate was reduced subsequently due to the suppression of FeO formation by the presence of chromium, Fe_3O_4 and Fe_2O_3 being far more protective. The oxidation rate was reduced progressively by addition of chromium greater than 1.25 wt %. If the chromium content in the steel is sufficiently high, the formation of wüstite is prevented above 570° C [33]. In the report of Wood *et al.* [32], an FeO layer could form until the chromium concentration reached about 2.5 wt %, but the primary cause of the reduced oxidation rate was the development of Fe–Cr spinel next to the base metal. The oxidation of FeO to Fe_3O_4 resulted in the formation of voids above the spinel layer. These led to the lifting of the outer iron oxide scale and a consequent reduction in oxidation rate. Cracking of those separated layers might cause a temporary increase in the oxidation rate. In general, chromium alone affects the oxidation similar to aluminium as described above. However, the suppression of FeO formation plays more important role than Fe–Al low alloys.

In dilute Fe–Cr alloys, it is not clear whether the spinel $FeCr_2O_4$ forms by itself or from the reaction of FeO with Cr_2O_3. It is thought that the spinel is less protective than pure Cr_2O_3 at high temperatures, but they are both effective at 700° C [23]. Iron containing 0.6 wt % Cr is less protective in air at 500 and 700° C than the one with 0.5 wt % Al [24] and there is a strong tendency for chromium-containing scales to spall on cooling which renders the scale less protective under cyclic conditions. Hammar *et al.* [34, 35] found that additions of less than 2 wt % Cr suppressed the oxidation properties of iron in oxygen at 625 and 675° C, while at 500 and 575° C such effect was very little. It was explained that below 570° C if the oxidized iron contains only small amounts of chromium, it will be dissolved as Cr^{3+} in the magnetite phase, the ions occupying octahedral sites. There will, therefore, be no difference in the vacancy concentration in the oxide phase due to the chromium ions.

In ternary alloys, von Fraunhofer and Pickup [24] reported that Fe–Cr–Si alloy oxidized faster than Fe–Al–Si alloy of similar amounts of alloying elements because the rate of oxide formation of the former alloy was slower and therefore more oxidation had occurred before protection was established. Furthermore, the scale on the Fe–Cr–Si alloy was markedly less adherent than that on the Fe–Al–Si alloy, and one can expect that it will readily spall off if their oxidation test samples are thermally cycled. As described above, the minimum silicon content to form a continuous SiO_2 film in CO_2 + 1 vol % CO at 500° C is 2.6 wt %. However, addition of chromium can reduce the bulk silicon concentration required to form such continuous SiO_2 layer by lowering the solubility of oxygen at the alloy–scale interface and reducing the internal oxidation of silicon [27]. The quantitative chromium content required was not specified.

4.5. Nickel

In contrast to the foregoing alloying elements (aluminium, silicon, and chromium), nickel is more noble than iron. Consequently, the iron matrix of nickel steel is selectively oxidized and nickel is rejected at the oxide–base metal interface [36]. Since the diffusion coefficient of nickel in iron is low, nickel does not diffuse rapidly back into the core and its concentration becomes much higher at the interface than in the core. Even in relatively dilute Fe–Ni alloys, the nickel concentration just ahead of this interface can be very high. For example [37], nickel enrichment in the Fe–1 wt % Ni alloy surface oxidized in oxygen at 1000° C almost approached 70 wt %. This selective oxidation of iron and concentration of nickel in a thin layer results in interpenetration of the oxide and metal at the interface and produces a tight mechanical oxide–metal bond and substantially increased oxidation resistance.

The typical scale that forms on a nickel steel consists of an outer layer of mainly iron oxides, an inner layer of oxides interspersed with a largely continuous three-dimensional filigree of nickel-rich metal [36], a very rough and indistinct oxide–metal interface, a zone in which large islands of iron-rich oxides are interspersed in a matrix of nickel-rich metal, and finally an inner zone of much smaller internal oxide particles where the more reactive residues such as silicon and chromium have precipitated as oxides within the steel.

4.6. Other elements

Other elements which are more noble than iron also tend to be rejected at the oxide–base metal interface. If the rate of diffusion of the element back into the core is higher than the oxidation rate, the concentration throughout the core gradually increases with no great build up at the surface. This can happen in the case of copper. However, at the high heating rates sometimes encountered in production, some of these elements can concentrate on the surface and cause interlocked tenacious scales similar to those characteristics of the nickel steels. A typical example of such beneficial effect of copper is the oxidation of iron alloyed with less than 2 wt % Cu in O_2 at 625° C [35].

Manganese can substitute for iron in the wüstite and magnetite lattices. Therefore, it was reported to attribute very slight effect alone on the oxidation of steel [38]. However, comparison of the experimental data [39] shows that mild steel (with 0.065 wt % C, $<$ 0.01 wt % Si, and 0.29 wt % Mn) oxidized slower than iron (with 0.006 wt % C) in air at 1000 and 1100° C probably due to the manganese content or the slight difference in carbon content. Furthermore, manganese together with silicon (in silicon-killed steels) can combine with iron oxide to form pools and extended stringers of iron–manganese–silicate in the scale layer. This can accelerate the scaling rate and may contribute to the formation of sticky scale. Manganese was also reported to promote the formation of spinels on heat-resistant steels, thereby helping the heat resistance [13].

Small amounts of phosphorus ($<$ 0.5 wt %) were shown to increase the resistance of iron to oxidation between 500 and 900° C, while at 1000° C a destructive effect was found [34, 40, 41]. However, at 500 and 625° C a beneficial effect culminated at a concentration of 0.1 wt % P, above which oxidation layers broke and became non-protective [40]. Below 900° C, the protection of phosphorus is to establish iron phosphate or phosphorous pentoxide, at the metal surface, both of which decompose or are gaseous above 950° C. The iron oxide film formed was thus separated from the metal and no protection was maintained at 1000° C [42]. However, the oxidation resistance of iron at 1000° C is increased when the phosphorus content exceeds 0.1 wt %, because gaseous iron phosphate is not thermally stable and is easy to transform to a stabilizing layer (iron phosphide) for protection. Addition of sufficient amount of copper (~ 0.33 wt %) will produce copper phosphide instead of iron phosphide, i.e. copper appears to act as a catalyst for the oxidation of phosphorus. Therefore, at 1000° C the combined effect of copper and phosphorus on the oxidation resistance of steel was beneficial, while at lower temperatures such beneficial effect was analogous to the effect of the elements separately [42].

With the exception of certain free-cutting steels with high sulphur contents, sulphur at the levels normally present in steel has no significant effect alone [38]. The effect of sulphur (0.006–0.5 wt %) on the oxidation properties of iron was also found to be very slight [43]. However, in the iron samples containing both 0.3 wt % Cu and various amounts of sulphur there existed a marked increase in the oxidation rate in argon + 20 vol % O_2 at 800° C when the sulphur content reached 0.11 wt % [44] at which sulphur exceeds the stoichiometric ratio of Cu_2S and the oxidation-preventing effect exerted by copper at the oxide–metal interface was thus removed.

Molybdenum is more noble than iron, and seems to behave like copper described above. However, experimental data concerning this effect are very few. A beneficial effect was reported by Inokuchi and Ito [45] that addition of 0.013 wt % Mo to a silicon steel produced a smooth surface and good oxidation resistance due to molybdenum concentrated near the surface and/or due to the fine molybdenum sulphide particles preventing grain boundary cracking. On the other hand, a detrimental effect was reported by Chelyshev *et al.* [46] that 0.45 wt % Mo in a Cr–Ni low alloy graphitized steel slightly increased oxidation sensitivity owing to formation of volatile MoO_3 type oxide which ruptured the oxide film and allowed access to atmosphere oxygen.

5. Effect of atmosphere on the oxidation

The furnace atmosphere for high temperature oxidation of steels consists of reaction products of the fuel such as N_2, H_2O, CO_2, H_2, CO, and SO_2 in proportions that depend on the air, fuel ratio, the composition of the fuel, and the temperature of the gas in the neighbourhood of the steel. Nitrogen is inert and its principal effect on the oxidation is dilution of other effective gaseous species only.

Generally speaking, H_2O and CO_2 are oxidizing gases. Their reactions with iron are as follows.

$$Fe + H_2O \rightarrow (FeO, Fe_3O_4) + H_2$$

$$Fe + CO_2 \rightarrow (FeO, Fe_3O_4) + CO$$

On the contrary, H_2 and CO are reducing gases

$$(FeO, Fe_3O_4) + H_2 \rightarrow Fe + H_2O$$

$$(FeO, Fe_3O_4) + CO \rightarrow Fe + CO_2$$

In high temperature oxidation the outward movement of iron ions from the metal through the scale to the reaction site often induces gaps at the scale–base metal interface. When the oxidation occurs in pure oxygen or in dry mixtures of oxygen and inert gases, the rate decreases because of the throttling action of the gaps upon the flux of iron ions through the scale as mentioned above. However, if sufficient water vapour or CO_2 is present in the atmosphere, the oxidation rate is maintained in spite of the gaps in the scale. The most probable explanation of the effect of H_2O and CO_2 is that these compounds transport oxygen across the gaps from the inner surface of the scale to the metal surface, where it dissociates. The oxygen ions released by the dissociation are adsorbed on the metal surface and react to form new scale. $H_2O \rightarrow H_2 + O_{\mathrm{adsorbed}}$ or $CO_2 \rightarrow CO + O_{\mathrm{adsorbed}}$. The hydrogen or carbon monoxide released by the dissociation migrates out to the inner surface of the scale. Here iron oxide is reduced by H_2 or CO. $H_2 + FeO \rightarrow Fe^{2+} + H_2O + 2e^-$ or $CO + FeO \rightarrow Fe^{2+} + CO_2 + 2e^-$ and H_2O or CO_2 is returned to the atmosphere in the gap to repeat the cycle. The iron ions produced by the reaction diffuse by means of lattice defects in the scale toward the scale/gas interface, site of the primary oxidation reaction. Fig. 3 is a schematic representation of this explanation proposed by Rahmel and Tobolski [47].

Two other mechanisms are also suggested. One was proposed by Surman and Castle [48] to explain the oxidation of iron and mild steel in steam below 570° C. These authors suggested vapour–phase diffusion of volatile $Fe(OH)_2$ from the oxide–metal interface to the outer layer oxide crystals. The dissociation products of H_2O permeate the scale. Iron is oxidized to $Fe(OH)_2$, carried outward in that form, and deposited as oxide at the outer part of the gap. The other one was proposed by Fujii and Meussner [49], and states that hydrogen from the dissociation of water vapour permeates the scale. Iron oxide is reduced by hydrogen at the outer part of the gap to produce water vapour, which then diffuses to the inner part of the gap and oxidized fresh iron.

The oxidation rate in $H_2O + O_2$ or $CO_2 + O_2$ atmosphere increases with increasing content of H_2O or CO_2, but a saturation value exists. For example [47], in the oxidation of iron at 950° C, the H_2O and CO_2 contents to attain saturation were reported to be 15 vol % and 12 vol % respectively. Tuck *et al.* [50] also found that iron and mild steel oxidized faster in 88 vol % O_2 + 12 vol % H_2O than in dry oxygen. In the mixture of $H_2O + H_2$ or $CO_2 + CO$ the oxidation rate decreases with increasing H_2 or CO content (reducing gas) and eventually the oxidizing efficiency will disappear at a certain proportion [51]. Further-

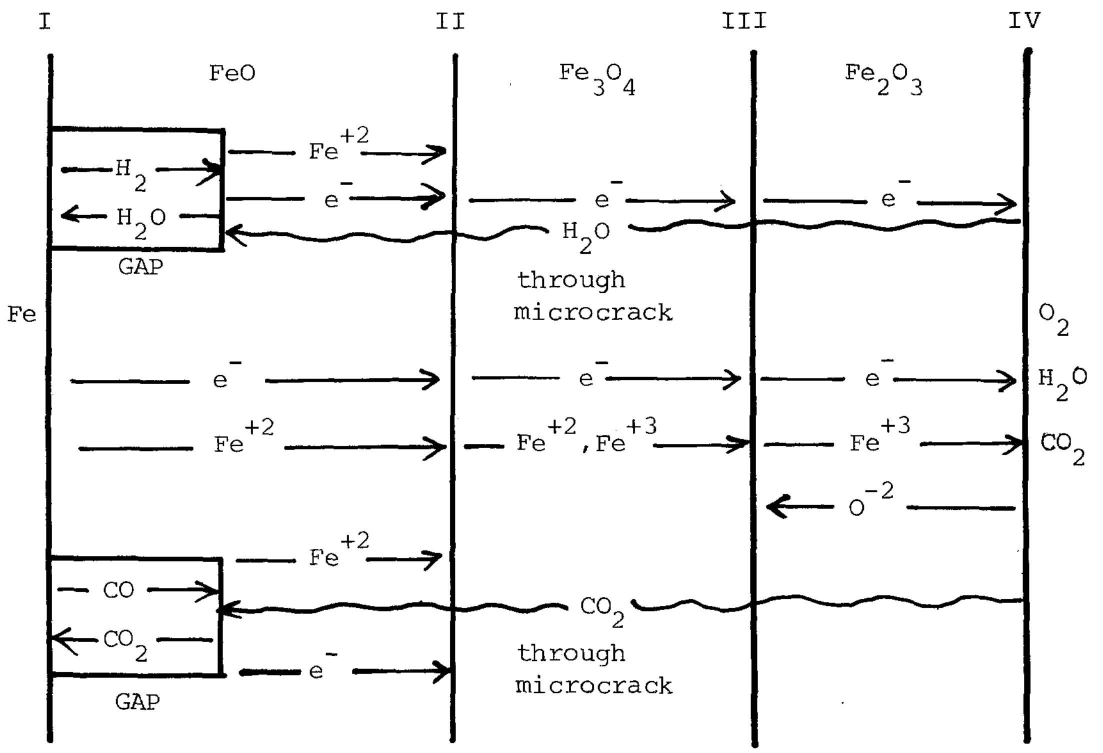

Figure 3 Mechanism of the oxidation of iron in atmospheres containing H_2O and CO_2 as suggested by Rahmel and Toboski [47].

more, the oxidation rate in pure oxygen is higher than that in dry air due to its higher oxygen partial pressure.

Sulphur dioxide tends to increase the oxidation rate. The main mechanism appears to be the formation of a liquid phase such as FeS in the scale and enhanced ionic transport through the scale. However, in the amounts normally present in industrial furnace its effect is marginal. In reducing atmospheres a sulphide phase is formed and grows very rapidly. In oxidizing atmospheres increasing the air–fuel ratio dilutes the SO_2 and minimizes its effect on the scale. A typical example is shown in Fig. 4 [39] which shows that above 4 vol % free oxygen, SO_2 has virtually no effect; the rate of oxidation accelerates rapidly with diminishing oxygen content, in sharp contrast to the effect in the absence of SO_2. A review paper concerning the oxidation of iron in atmospheres containing SO_2 was published early in 1971 [52]. However, such information of low alloy steels is rarely reported.

The rate of delivery of the oxidizing species to the surface of the steel depends not only on the composition of the atmosphere but also on the flow rate. The effect of gas speed on oxidation rate was reviewed in 1967 [53]. The overall summary is that the oxidation rate increases with gas flow up to a critical flow rate, and then remains constant. However, some workers did not find significant effect of the air speed on the oxidation rate, because the actual critical air speed is not in the range of air speed they investigated. Investigations in such effect are very few after 1967.

6. Effect of cold work on the oxidation

Rough surfaces of iron oxidize at a lower rate than smooth surfaces [8, 54] due to the formation of porous scales on rough surfaces, retarding the diffusion of iron ions. Cold work, induced by mechanical polishing of surfaces, enhances the oxidation rate in air or oxygen by mopping up cation vacancies diffusing through the scale toward the metal [55], because cold work produces extra dislocations which act as vacancy sinks and inhibit the formation of cavities. In addition, cold work enhances initially the diffusion of ions through the scale and promotes the oxidation rate. Impurities increase the oxidation rate of cold worked iron by increasing the cold work effect and by the persistence of that effect. At temperatures higher than 600° C recrystallization occurs very fast so that cold worked specimens behave in essentially the same way as annealed specimens and oxidize at the same rates [56]. At lower temperature ($\sim 400°$ C), however, cold work persists for the initial stages of oxidation, so that vacancies can be readily removed and void formation will not occur; the oxidation rate for cold worked iron will thus be greater than that for annealed material.

7. Conclusion

In conclusion, high temperature oxidation of low alloy steels are summarized as follows.

(i) From the Fe–O phase diagram, one can foretell the kinds of oxides exist at a certain temperature. For example, FeO, Fe_3O_4, and Fe_2O_3 might exist above 570° C, while only Fe_3O_4 and Fe_2O_3 exist below this temperature.

(ii) Iron oxidation consists mainly of the outward diffusion of iron ions and the inward diffusion of oxygen ions. One can determine the rate-controlling step from the measurement of the oxidation rate in oxidation kinetics. Therefore, essentially three types of rate laws are observed in high temperature oxidation: parabolic, linear, and intermediate.

(iii) The main effect of alloying elements less noble than iron, such as aluminium, silicon, chromium, on the oxidation is the formation of a protective layer,

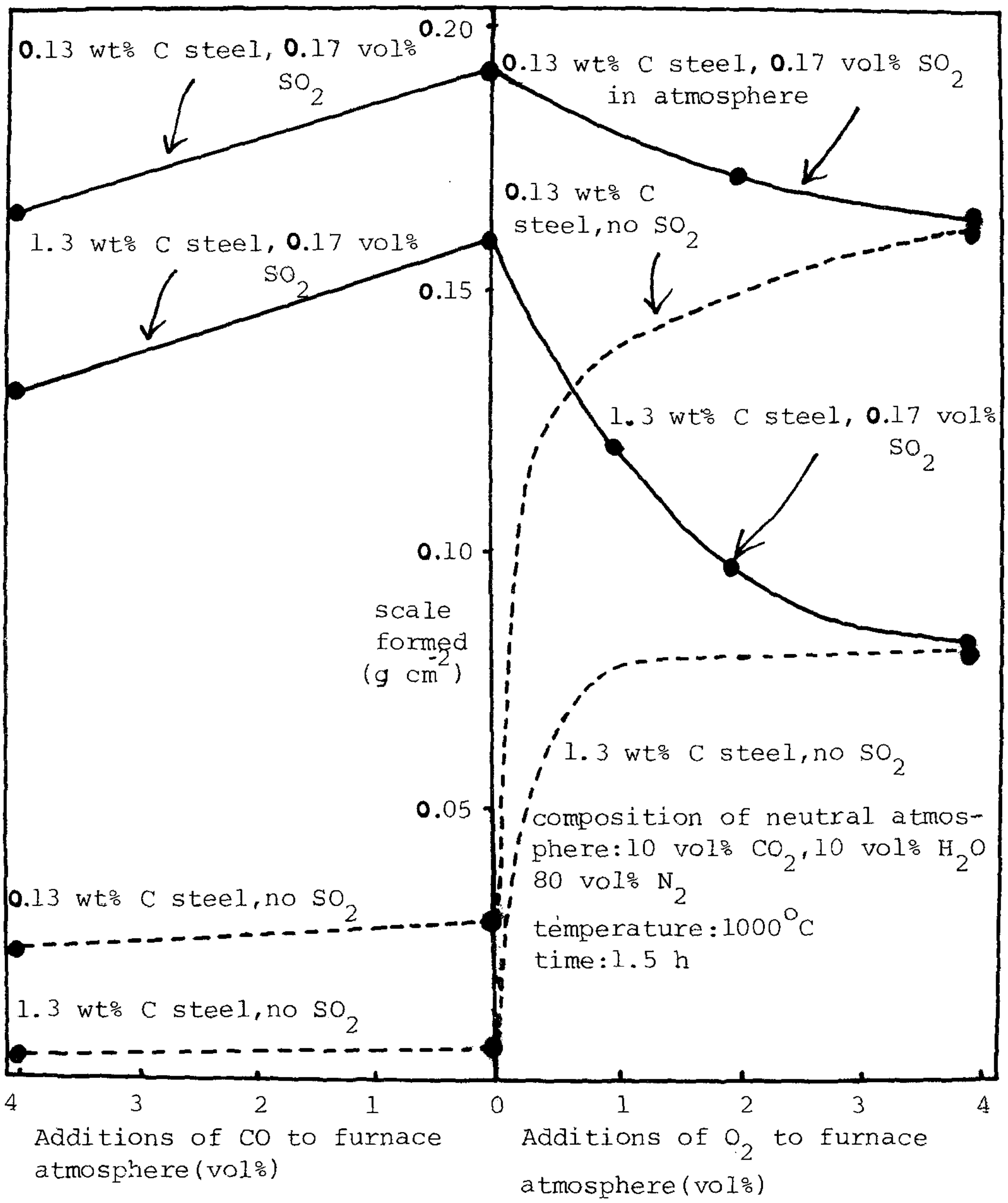

Figure 4 Influence of additions of Co and O_2 to the atmosphere containing 0.17 vol % SO_2 and to that free from SO_2 on the oxidation of plain carbon steel [39].

enriched in alloying elements, at the scale–base metal interface, although some other mechanisms (e.g. the inhibition of wüstite formation) might also be possible. However, among the three, silicon is the most protective element, while chromium is the least. On the other hand, those elements more noble than iron, such as nickel, copper, are to be rejected at the scale–base metal interface, acting as a tight mechanical bond and increasing the oxidation resistance. However, from the thermodynamic viewpoint and from this review, the less noble elements seem better than the more noble elements to act as alloying elements for development of high temperature oxidation resistant low alloy steels. Some protective layers are produced from the combined effect of more than one alloying element (e.g. phosphorus and copper). The effect of carbon on the oxidation depends on whether it facilitates or hinders the transport of diffusing ions.

(iv) Oxidizing gases, such as H_2O and CO_2, can promote the oxidation of steels, while reducing gases, such as H_2 and CO, can inhibit the oxidation. SO_2 tends to increase the oxidation rate. However, the more oxidizing the atmosphere is, the less such effect behaves significantly.

(v) The effect of cold work is to inhibit the formation of cavities as well as to enhance the initial iron ion diffusion. Therefore, the oxidation in air or oxygen is increased.

References

1. O. KUBASCHEWSKI and B. E. HOPKINS, in "Oxidation of Metals and Alloys", 2nd edn, Butterworths, London (1962).
2. PER KOFSTAD, in "High Temperature Oxidation Of Metals", Wiley, New York (1966).
3. J. W. HICKMAN and E. A. GULBRANSEN, *Trans. AIME* **171** (1947) 344.
4. G. CHAUDRON and H. FORESTIER, *Acad. Sci.* **178** (1924) 2173.
5. W. A. FISHER, A. HOFFMANN and R. SHINADA, *Arch. Eisenh.* **27** (1956) 521.
6. S. SHIRAIWA and N. MATSUNO, *Sumitomo Met.* **19** (1967) 33.
7. H. J. ENGELL and F. WEVER, *Acta Metall.* **5** (1957) 695.
8. J. A. VON FRAUNHOFER and G. A. PICKUP, *Corros. Sci.* **10** (1970) 253.

9. "CRC Handbook of Chemistry and Physics", 66th edn, CRC Press, Cleveland, Ohio (1985).
10. P. S. LU and C. H. HUANG, *Mater. Sci. Quart.* **6** (1974) 40.
11. K. HAUFFE, *Metalloberfläche* **8** (1954) 97.
12. F. GESMUNDO and F. VIANI, *Corros. Sci.* **18** (1978) 217, 231.
13. A. RAHMEL, *Chem. Metall. Iron Steel* **146** (1973) 395.
14. W. H. AILOR (ed.), in "Handbook On Corrosion Testing and Evaluation", Wiley, New York (1971) p. 291.
15. U. R. EVANS (ed.), in "The Corrosion and Oxidation Of Metals", Edward Arnold, London (1977) Chap. XX.
16. W. E. BOGGS and R. H. KACHIK, *J. Electrochem. Soc.* **116** (1969) 424.
17. D. CAPLAN, G. I. SPROULE, R. J. HUSSEY and M. J. GRAHAM, *Oxid. Met.* **12** (1978) 67.
18. *Idem, ibid.* **13** (1979) 255.
19. A. U. MALIK and D. P. WHITTLE, *Oxid. Met.* **16** (1981) 339.
20. F. I. WEI, K. H. CHENG and J. Y. WU, "The Study Of Scaling Mechanism Of CSC Rod & Bar", China Steel Corporation Report PJ-70-003 (1981).
21. E. I. KOROCHKIN, A. A. KALINICHEV and A. A. BORISOVSKII, *Steel USSR* **1** (1971) 668.
22. F. SAEQUSA and L. LEE, *Corrosion* **22** (1966) 168.
23. J. B. NEWKIRK (ed.), in "High Temperature Materials Coatings and Surface Interactions", Freund, Tel-Aviv, Israel (1980) p. 1.
24. J. A. VON FRAUNHOFER and G. A. PICKUP, *Anti-Corros.* **17** (1970) 10.
25. Z. Z. HUANG and R. Z. ZHU, *Proc. JIMIS* **3** (1983) 231.
26. L. S. DARKEN, *Trans. AIME* **150** (1942) 157.
27. A. ATKINSON, *Corros. Sci.* **22** (1982) 87.
28. C. W. TUCK, *ibid.* **5** (1965) 631.
29. W. W. SMELTZER, L. A. MORRIS and R. C. LOGANI, *Can. Metall. Quart.* **9** (1970) 513.
30. P. A. GERMAN and A. C. LITTLEJOHN, in "Corrosion of Steels in CO_2", BNES Conference Proceedings, Reading University, Berkshire, UK (1974) p. 1.
31. W. F. JEPSON and G. W. LORIMER, *Environ. Degradation High Temp. Mater.* **2** (1980) 5.
32. G. C. WOOD, I. G. WRIGHT, T. HODGKIESS and D. P. WHITTLE, *Workstoffe Korrosion* **21** (1970) 900.
33. D. MORTIMER and W. B. A. SHARP, *Brit. Corros. J.* **3** (1968) 61.
34. B. HAMMAR, L. JANSSON, I. SVEDUNG and N. G. VANNERBERG, in 6th Scandanavian Corrosion Congress (Foundation of Scientific and Industrial Research, 1971) No. 7.
35. B. HAMMAR and N. G. VANNERBERG, *Scand. J. Metall.* **3** (1974) 123.
36. G. G. BROWN and K. G. WOLD, *JISI* **207** (1969) 1457.
37. G. L. WULF, T. J. CARTER and G. R. WALLWORK, *Corros. Sci.* **9** (1969) 689.
38. T. SMITH, *Steel Times* **210** (1982) 339.
39. K. SACHS and C. W. TUCK, Proceedings of Conference on "Reheating for hot working" (ISI, London, 1967) p. 1.
40. N. G. VANNERBERG and I. SVEDUNG, *Corros. Sci.* **11** (1971) 915.
41. I. SVEDUNG and N. G. VANNERBERG, *Scand. J. Metall.* **1** (1972) 141.
42. I. SVEDUNG, R. POMPE and N. G. VANNERBERG, *ibid.* **5** (1976) 129.
43. B. HAMMAR and N. G. VANNERBERG, *ibid.* **3** (1974) 173.
44. B. HAMMAR and N. G. VANNERBERG, in 7th Scandanavian Corrosion Congress, 1975, (Foundation of Scientific and Industrial Research, Trondheim, Norway) p. 137.
45. Y. INOKUCHI and Y. ITO, *Bull. Jpn Inst. Met.* **23** (1984) 276.
46. N. A. CHELYSHEV, F. I. ARDOVSKII and L. V. SHCHEKURSKAYA, *Steel USSR* **12** (1982) 483.
47. A. RAHMEL and J. TOBOLSKI, *Corros. Sci.* **5** (1965) 333.
48. P. L. SURMAN and J. E. CASTLE, *ibid.* **9** (1969) 771.
49. C. T. FUJII and R. A. MEUSSNER, *J. Electrochem. Soc.* **111** (1964) 1215.
50. C. W. TUCK, M. ODGERS and K. SACHS, *Corros. Sci.* **9** (1969) 271.
51. P. KOFSTAD and R. BREDESEN, in International Congress Metallic Corrosion (Proceedings Conference), Toronto, Canada, June 1984, p. 12.
52. T. FLATLEY and N. BIRKS, *JISI* July (1971) 523.
53. C. W. TUCK and D. W. DOWN, *ibid.* Sept. (1967) 972.
54. L. JANSSON and N. G. VANNERBERG, *Oxid. Met.* **3** (1971) 453.
55. D. CAPLAN, G. I. SPROULE and R. J. HUSSEY, *Corros. Sci.* **10** (1970) 9.
56. W. R. PRICE, *ibid.* **7** (1967) 477.

Received 7 December 1987
and accepted 16 March 1988